The Plant Cell, Vol. 20: 1029–1039, April 2008, www.plantcell.org © 2008 American Society of Plant Biologists

Thylakoid Membrane Remodeling during State Transitions in *Arabidopsis* [W]

Silvia G. Chuartzman,[a] Reinat Nevo,[a] Eyal Shimoni,[b] Dana Charuvi,[a,c] Vladimir Kiss,[a] Itzhak Ohad,[d] Vlad Brumfeld,[e,1] and Ziv Reich[a,1]

[a] Department of Biological Chemistry, Weizmann Institute of Science, Rehovot 76100, Israel
[b] Electron Microscopy Unit, Weizmann Institute of Science, Rehovot 76100, Israel
[c] Robert H. Smith Institute of Plant Sciences and Genetics in Agriculture, Hebrew University of Jerusalem, Rehovot 76100, Israel
[d] Institute of Life Sciences and Avron-Even-Ari Minerva Center for Photosynthesis Research, Hebrew University of Jerusalem, Jerusalem 91014, Israel
[e] Department of Plant Sciences, Weizmann Institute of Science, Rehovot 76100, Israel

Adaptability of oxygenic photosynthetic organisms to fluctuations in light spectral composition and intensity is conferred by state transitions, short-term regulatory processes that enable the photosynthetic apparatus to rapidly adjust to variations in light quality. In green algae and higher plants, these processes are accompanied by reversible structural rearrangements in the thylakoid membranes. We studied these structural changes in the thylakoid membranes of *Arabidopsis thaliana* chloroplasts using atomic force microscopy, scanning and transmission electron microscopy, and confocal imaging. Based on our results and on the recently determined three-dimensional structure of higher-plant thylakoids trapped in one of the two major light-adapted states, we propose a model for the transitions in membrane architecture. The model suggests that reorganization of the membranes involves fission and fusion events that occur at the interface between the appressed (granal) and nonappressed (stroma lamellar) domains of the thylakoid membranes. Vertical and lateral displacements of the grana layers presumably follow these localized events, eventually leading to macroscopic rearrangements of the entire membrane network.

INTRODUCTION

The two photosystems that mediate electron transport in oxygenic photosynthesis are connected electrically in series. However, they have different absorption characteristics and exciton trapping efficiencies, necessitating a means to balance electron flow between them under varying light conditions. In vivo, this tuning ability is provided by rapid-response adaptation processes called state transitions. In the so-called state I, which is observed in darkness or under light conditions favorable for photosystem I (PSI), the light-harvesting antenna complex II (LHCII) is associated primarily with photosystem II (PSII). If light changes such that PSII is excited preferentially (state II), a fraction of LHCII becomes phosphorylated by dedicated kinase(s). Activation of the latter is driven by the intersystem electron mediator, cytochrome b_6f, and is governed by the redox state of the plastoquinone pool, which becomes more reduced under conditions that favor state II. The phosphorylated fraction of LHCII then dissociates from PSII and binds to PSI, thus increasing the latter's ability to harvest light at the expense of the former. Reversal of light conditions back to state I results in inactivation of the kinase(s), and the LHCII antennae become dephosphorylated by constitutively active phosphatases. Subsequently, the (dephosphorylated) LHCII complexes reassociate with PSII, restoring its original capacity to absorb light (Allen, 1992a, 1992b; Allen and Forsberg, 2001; Haldrup et al., 2001; Kruse, 2001; Wollman, 2001; Aro and Ohad, 2003; Mullineaux and Emlyn-Jones, 2005; Rochaix, 2007).

In higher plants and other chloroplast-bearing organisms whose thylakoid membranes are differentiated into grana and stroma lamellar domains, the movement of LHCII between granal-localized PSII and stroma lamellar-residing PSI is expected to lead to structural changes in the grana because LHCII is a major stabilizer of appressed granal domains (Anderson, 1999; Garab and Mustardy, 1999; Dekker and Boekema, 2005). However, the magnitude of these changes is under dispute. Based on results obtained from subjecting isolated thylakoids to low-salt solutions (Izawa and Good, 1966; Murakami and Packer, 1971), which presumably mimic state I → state II transitions, it had been proposed that the movement of LHCII from the grana to the stroma lamellae leads to massive structural rearrangements in the grana to the extent of complete unstacking of the appressed layers (Ryrie, 1983; Arvidsson and Sundby, 1999). Other views, however, hold that the changes in membrane organization during light-induced state transitions in vivo are of much more limited nature and are mostly confined to the grana margins (see Drepper et al., 1993; Mustardy and Garab, 2003; Shimoni et al., 2005).

The issue of shape transitions of thylakoid membranes is further complicated by a recent work showing that the granum-stroma

[1] Address correspondence to vlad.brumfeld@weizmann.ac.il or ziv.reich@weizmann.ac.il.
The author responsible for distribution of materials integral to the findings presented in this article in accordance with the policy described in the Instructions for Authors (www.plantcell.org) is: Ziv Reich (ziv.reich@weizmann.ac.il).
[W] Online version contains Web-only data.
www.plantcell.org/cgi/doi/10.1105/tpc.107.055830

assembly of higher-plant chloroplasts is highly interconnected (Shimoni et al., 2005). Using electron microscope tomography, we showed that, in dark-adapted chloroplasts, the granum layers are formed by bifurcations of stroma lamellar sheets that fuse within the granum body. In addition to these lateral connections, adjacent layers are fused to each other through membrane bridges that are located at the edges of the granum body. Thus, any significant alteration in the structure of the assembly requires breakage of the lateral and/or vertical connections in the assembly.

In this work, we combined several microscopic techniques to study the morphological changes that occur in thylakoid membranes of higher plant chloroplasts during state transitions. We found that the rearrangements in membrane architecture occurring during the transitions are large scale, involving both granal and stroma lamellar domains. Remodeling of the membranes during state I → state II transition is initiated at the highly curved margins of the appressed granal domains and involves breakage of the aforementioned lateral and/or vertical connections that stabilize the granum-stroma assembly. Following these localized rearrangements, the grana undergo a macroscopic, probably cooperative, transition that then propagates throughout the entire network. The fission events that accompany the transition from state I to state II, as well as the fusion events that must occur during the reverse reaction, may require the participation of dedicated machinery like the ones operating in the mitochondria or in the Golgi apparatus.

RESULTS

Due to the inherent structural complexity of the chloroplast thylakoid membranes, we used a number of high-resolution imaging methods for our analyses. Imaging of thylakoids by two of these, atomic force microscopy (AFM) and scanning electron microscopy, which are surface imaging techniques, required that the two envelope membranes of the chloroplast be removed. Therefore, in all studies we used de-enveloped chloroplasts whose thylakoid network is structurally intact and photochemically active (Casazza et al., 2001; Kaftan et al., 2002). These thylakoids were able to support the entire chain of electron transport, from H_2O to $NADP^+$, with an oxygen evolution rate of 73 ± 10 μmol $O_2 \cdot mg^{-1}Chl \cdot h^{-1}$, within the range reported for isolated thylakoids (Casazza et al., 2001). The maximum photochemical yield of PSII, Φ_p^{max}, measured for the samples, was 0.68 ± 0.02, close to the value measured in intact leaves (Maxwell and Johnson, 2000).

State I–adapted thylakoids isolated from dark-adapted plants were used either directly or after exposure to 100 μmol photons·$m^{-2} \cdot s^{-1}$ of PSI-specific light (λ_{max} = 740 nm) for 30 min. To induce state II, thylakoids were exposed to 15 to 200 μmol photons·$m^{-2} \cdot s^{-1}$ of PSII-specific light (λ_{max} = 640 nm) for 5 to 30 min or to different concentrations of duroquinol (in the dark), which directly reduces the plastoquinone pool. The extent of the transitions was evaluated by monitoring the phosphorylation levels of the LHCII proteins Lhcb1 and Lhcb2. Maximal levels were obtained when the thylakoids were exposed to 30 μmol photons·$m^{-2} \cdot s^{-1}$ for 30 min or when treated with 1 mM duroquinol (Figure 1A), with the latter resulting in higher levels.

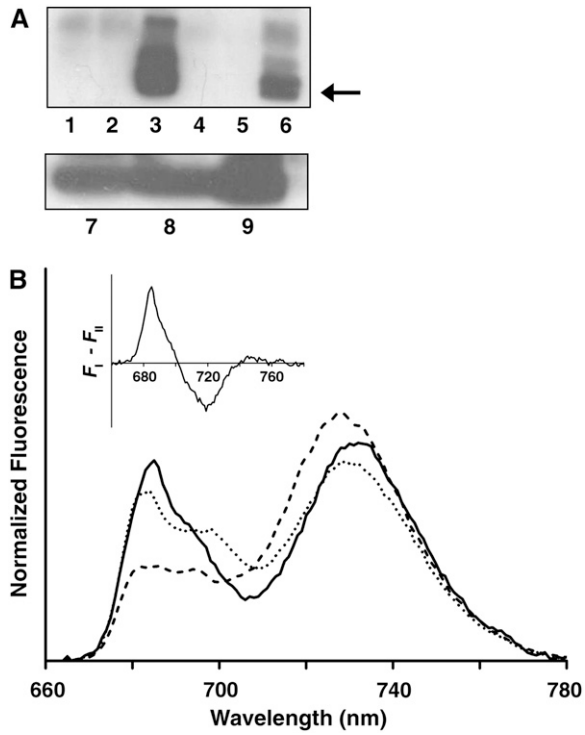

Figure 1. Induction of State I → State II Transition in De-Enveloped Chloroplasts.

(A) Transitions monitored by detecting the level of phosphorylated Lhcb1/2. Anti-phosphothreonine was used to probe immunoblots of the following thylakoid preparations. Lanes 1 to 6: thylakoids that were dark-adapted (1), dark-adapted with ATP (2), treated with duroquinol plus ATP (3), subjected to 30 μmol photons·$m^{-2} \cdot s^{-1}$ of 640-nm light for 30 min without ATP (4), or with ATP in the presence (5) or absence of 10 μM DCMU (6). Lanes 7 to 9: thylakoids subjected to 30 μmol photons·$m^{-2} \cdot s^{-1}$ of 640-nm light for 5, 10, or 30 min, respectively.
(B) Transitions monitored by low-temperature chlorophyll fluorescence measurements. The emission spectra shown were recorded at 77K using an excitation wavelength of 480 nm. Spectra were normalized to the area below the curves. Thylakoids were trapped in state I (solid line) and then induced to undergo two sequential transitions: first to state II (dashed line) and subsequently back to state I (dotted line). The increase of the 730-nm peak upon exposure to PSII-specific light is indicative of the association of LHCII with PSI. Inset: Fluorescence difference spectrum ($F_I - F_{II}$). The area below the positive and negative peaks is approximately the same, as expected.

Adaptation of the thylakoids to the two states was also assessed by chlorophyll fluorescence measurements. Low-temperature (77K) fluorescence showed that thylakoids adapted to state I gave rise to spectra in which PSI and PSII contribute roughly equally to the emitted fluorescence (Figure 1B, solid line). As expected, when state II was induced, PSI fluorescence (730 nm) increased markedly (Figure 1B, dashed line), indicative of the redistribution of excitation energy between the two PSs due to association of LHCII with PSI. State transitions were also monitored at room temperature by pulse amplitude modulation fluorescence measurements (see Supplemental Figure 1 online).

For the isolated thylakoids used in this study, transition to state II was accompanied by ~20% decrease of F_m. As expected, no significant change of F_m in the absence of ATP was observed.

Figure 2 shows AFM images of de-enveloped chloroplasts adapted to state I (Figure 2A) or state II (Figure 2B). In this and following structural analyses, state II was induced by exposure to 30 μmol photons·m^{-2}·s^{-1} for 30 min or to 1 mM duroquinol (in the dark). The transition from state I to state II was accompanied by a substantial increase in chloroplasts' diameter concomitant with a significant decrease in height (Table 1), resulting in a gain in ellipticity or, more appropriately, in oblateness. On a smaller scale, the transition between the two states caused the grana (which appear as bright spots in the topographs) to become less defined (cf. Figures 2C and 2E with 2D and 2F). The latter effect was particularly apparent in thylakoids that were induced to undergo transition to state II by duroquinol (Figure 2F), in correlation with the extent of LHCII phosphorylation (Figure 1A). Subjecting state I–adapted chloroplasts to PSII-specific light in the absence of ATP had no detectable effect on their morphology (Figure 2E, Table 1).

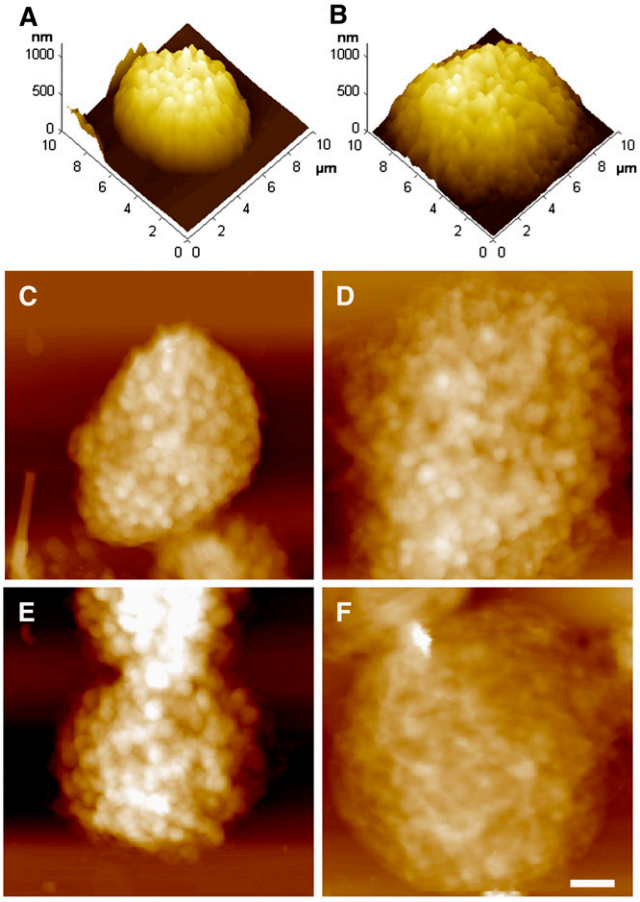

Figure 2. AFM Images of De-Enveloped Chloroplasts Trapped in State I or State II.

(A) and **(B)** Three-dimensional rendering of state I **(A)** and state II **(B)** adapted thylakoids.

(C) to **(F)** Height images of thylakoids subjected to different treatments. All samples, except **(E)**, were incubated in the presence of 1 mM ATP and 10 mM NaF. Bar = 1 μm.

(C) A dark-adapted chloroplast.

(D) and **(E)** Dark-adapted chloroplasts exposed to PSII-specific light in the presence **(D)** or absence **(E)** of ATP.

(F) A dark-adapted chloroplast induced to undergo transition to state II by treatment with 1 mM duroquinol (in the dark).

Table 1. Geometrical Parameters Derived from Surface Analysis of State I– and State II–Adapted De-Enveloped Chloroplasts

Treatment	Chloroplast Height (nm)	Chloroplast Base Area (μm^2)	Area of Grana End Membranes (nm^2)
Dark adaptation	754 ± 26	33 ± 2	(207 ± 7) × 10^3
640-nm light (+ATP)	581[a] ± 27	48[a] ± 2	(141[a] ± 4) × 10^3
Duroquinol (+ATP)	516[a] ± 47	42[a] ± 3	ND
640-nm light (−ATP)	688 ± 43	28 ± 2	(202 ± 7) × 10^3

Details of the statistical analysis are provided in Methods. Data are shown as the mean ± SE. ND, not determined (see text).

[a] Values significantly different from those determined for untreated dark-adapted chloroplasts (state I).

The surface topography of the thylakoids was also studied by scanning electron microscopy. As evident from the AFM images, the transition from state I to state II led to an increase in the chloroplasts' base area (Figures 3A and 3B, Table 1). The micrographs also revealed that the transition was accompanied by a considerable loss of granum structure, consistent with unstacking and disassembly of the grana during the process (Figures 3C and 3D). Grana that could still be discerned over the thylakoid surface in state II were smaller, with the area of their end membranes averaging at (141 ± 4) × 10^3 nm^2 compared with (207 ± 7) × 10^3 nm^2 in state I (Table 1). Induction of state II by duroquinol caused massive disassembly of the grana, which precluded analysis of their size. It has been shown that light-induced conformational changes in LHCII limit the accessibility of the kinase to the phosphorylation sites, either directly or by promoting aggregation of LHCII complexes (Zer et al., 2003). The extensive damage caused to the membranes in samples treated with duroquinol in the dark highlights the importance of this light-dependent inhibitory mechanism.

The above results indicate that the transitions between the two chromatic states of the thylakoid membranes are accompanied by large-scale changes in network architecture. However, the analyses used are surface techniques and thus cannot provide information on the underlying rearrangements in granum and stroma lamellar structure. To follow the changes occurring within the chloroplast volume during the transitions, thylakoids were subjected to cross-sectional analysis by transmission electron microscopy. Dark-adapted de-enveloped chloroplasts were examined first, allowing for comparison with the structure we determined by electron tomography for chloroplasts within leaves at the same illumination conditions (Shimoni et al., 2005). Albeit missing their envelope membranes, the morphology of these chloroplasts was generally similar to that of the intact chloroplasts. The thylakoid membranes exhibited the characteristic differentiated pattern with cylindrical stacked structures,

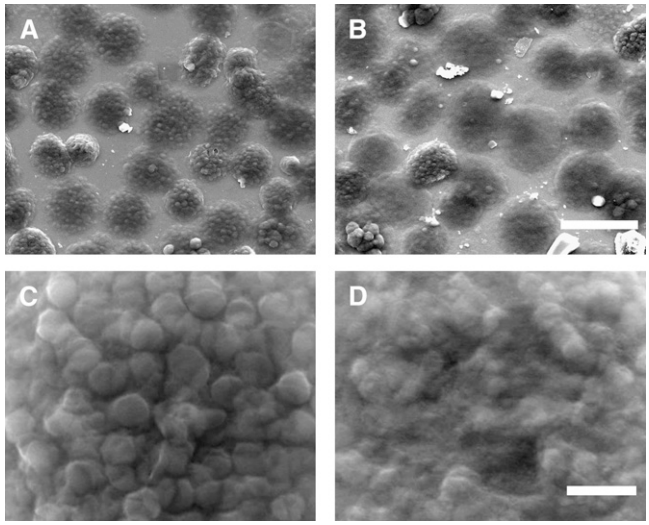

Figure 3. Scanning Electron Microscopy Images of State I– and State II–Adapted De-Enveloped Chloroplasts.

(A) and **(B)** Low-magnification overview of de-enveloped chloroplasts adapted to state I **(A)** or state II **(B)**. Bar = 10 μm.
(C) and **(D)** Close-up images showing surface details of a chloroplast adapted to state I **(C)** or state II **(D)**. The protruding discs apparent on the surface of the chloroplast shown in **(C)** are grana. Bar = 1 μm.

the grana, interconnected by multiple strips of unstacked, roughly parallel paired membranes—the stroma lamellae (Figures 4A and 4B). The number of layers within the grana varied between 2 and 15, averaging 6. Taking the distance between the surfaces of neighboring discs as ~4 nm (Shimoni et al., 2005), we calculated the average thickness of the layers to be 25 to 26 nm (Table 2), close to the values measured for isolated enveloped chloroplasts (Nir and Pease, 1973) and chloroplasts within leaves (Shimoni et al., 2005).

Upon transition to state II, the thylakoid membranes underwent substantial structural rearrangements, both on small and large scales. The small-scale rearrangments were mostly concentrated in the grana and involved various alterations in granum shape and connectivity. Specifically, the grana unstacked and transformed into loose, disordered structures that formed diffuse boundaries with the flanking stroma lamellae (Figures 4C and 4D), contrasting with the ordered, compact morphology observed in dark-adapted thylakoids. These structural rearrangements were accompanied by a decrease in the average number of layers in the stacks from 6 to 4 and by a marked swelling of the grana thylakoid lumen from 25 to 26 nm to 31 to 32 nm (Table 2). Underlying the alterations in granum structure were two processes, the first of which was separation of adjacent layers in the stacks. Such separation, which often involved large distances (i.e., up to a few tens of nanometers) led to unstacking of the grana (Figure 4D) and caused fragmentation of granum bodies into smaller-sized granal domains (Figure 4E). The second process involved displacement of layers outside the granum body, resulting in staggered, disordered morphologies (Figure 4F) and the emergence of hybrid structures that appeared halfway between granal and stromal thylakoids (Figure 4G). Importantly, none of the aforementioned processes could have taken place without breakage of some of the lateral and/or vertical connections that link the layers in the granum-stroma assembly in state I.

The extensive reorganization of the grana was accompanied by macroscopic changes in the thylakoid network. Owing to the partial disassembly of the granum-stroma assemblies, the network became less ordered and had lost its characteristic, highly differentiated morphology. It also underwent a significant expansion, in agreement with the results obtained from the AFM and scanning electron microscopy analyses, which showed a significant increase in network diameter following the transition to state II (cf. Figures 4C and 4A). Another prominent change in the network relates to the apparent stiffness of the membranes. In state II, the thylakoid membranes were frequently observed to

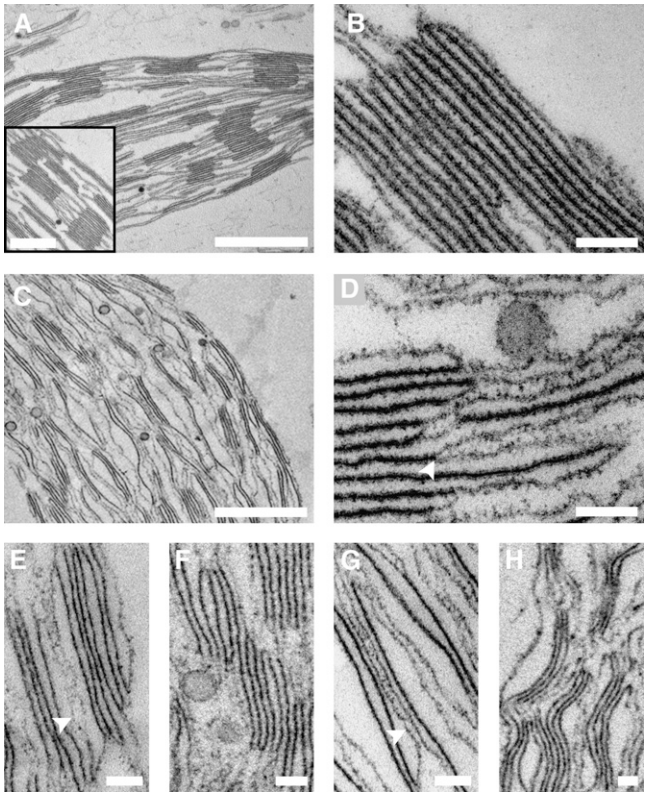

Figure 4. Cross-Sectional Analysis of State I– and State II-Adapted Thylakoid Membranes by TEM.

(A) and **(B)** Dark-adapted de-enveloped chloroplasts showing the complete thylakoid network **(A)** and a granum in detail **(B)**. Bars = 1 μm in **(A)**, 500 nm in the inset, and 100 nm in **(B)**.
(C) and **(D)** De-enveloped chloroplasts adapted to state II showing the complete thylakoid network **(C)** and a granum in detail (**[D]**; arrowhead indicates separation of adjacent layers). Bars = 1 μm in **(C)** and 100 nm in **(D)**.
(E) to **(H)** Distinctive features of the grana-stroma assembly in thylakoids adapted to state II. Arrowheads in **(E)** and **(G)** denote hybrid lamellae possessing features of both granal and stroma lamellar thylakoids. Bars = 100 nm.
All samples were incubated in the presence of 1 mM ATP and 10 mM NaF.

Table 2. Geometrical Parameters Derived from Cross-Sectional Analysis of State I– and State II–Adapted De-Enveloped Chloroplasts

Treatment	Diameter of the Grana (nm)	Thickness of Granum Layers (nm)
Dark adaptation	577 ± 18	25.2 ± 0.5
640-nm light (+ATP)	466[a] ± 14	31.6[a] ± 0.7
640-nm light (−ATP)	621 ± 17	27.5 ± 0.4

Details of the statistical analysis are provided in Methods. Data are shown as the mean ± SE.

[a] Values significantly different from those determined for untreated dark-adapted chloroplasts (state I).

adopt undulating morphologies, resulting in a distinctive wavy appearance (Figures 4C and 4H). This apparent increase in deformability may reflect a loss of interlayer attractions and/or enhanced (ionic) screening of surface charges, following the decrease in LHCII density due to its migration to the stroma lamellae. The latter may also disrupt interactions between the luminal domains of granal proteins, such as the PsbP and PsbQ subunits of PSII, which were proposed to attract the opposite faces of the granum layers toward each other (Dekker and Boekema, 2005). Disruption of these interactions is also expected to decrease the rigidity of the (paired) membranes and may account for the observed thickening or swelling of the grana thylakoids in state II.

To complement the AFM and electron microscopy analyses, which were performed on fixed specimen, we used confocal microscopy to follow the rearrangements in membrane organization in native-hydrated, unfixed de-enveloped chloroplasts. Here, we took advantage of the fact that the fluorescence emitted by thylakoid membranes at room temperature originates predominantly from PSII (Govindjee, 1995). State I–adapted thylakoids exhibited well-defined bright fluorescent spots marking granal domains, consistent with the confinement of PSII to these regions in this state (Figure 5A). Following exposure to PSII-specific light, the spots lost their boundaries and merged into large, diffuse fluorescent domains (Figure 5B). Spreading of the fluorescence in state II may be due to migration and subsequent dispersion of individual PSII molecules in the stroma lamellae. However, we believe that the changes in fluorescence reflect displacement of granum layers, along with their PSII-LHCII complexes, outside the granum core. This is in line with previous studies that showed that PSII molecular complexes do not mix in the stroma lamellae in state II–adapted thylakoids, but rather remain segregated in regions of an apparent granal origin (Staehelin and Van der staay, 1996).

Low-temperature fluorescence measurements (Figure 1B) indicate that the transitions between state I and state II, as assayed in our preparations, are largely reversible. Thus, we set out to determine whether this reversibility is also valid for the structural changes that accompany the transitions. For this, de-enveloped chloroplasts were either dark-adapted or trapped in state I and then induced to undergo two consecutive transitions, first to state II, and then back to state I. Here, state I was induced by subjecting the thylakoids to PSI-specific light in the presence of PSI electron acceptors in the medium (ferredoxin and $NADP^+$). This ensured that the LHCII kinase(s) are deactivated at the beginning of the cycle as well as at the onset of the second transition (state II → state I). In these experiments, we also included gramicidin D to prevent endogenous ATP production during the transitions. However, control experiments in the absence of this uncoupler gave rise to identical results.

In the first set of experiments, we followed the entire sequence of structural changes during the transitions in de-enveloped chloroplasts in real time by confocal microscopy (Figure 5E; see Supplemental Figure 2 online). The setup devised for this experiment is described in Methods. Dark-adapted thylakoids were induced to undergo transition to state II and then to state I and imaged throughout. The images clearly show the gradual disappearance of the bright spots that represent the granal domains during the transition to state II and their reappearance during the subsequent transition to state I. However, recovery of the granal domains was not complete. Notably, spreading of the fluorescent signal during the transition from state I to state II continued for ~20 min after the onset of illumination. This timescale is clearly too large to reflect diffusion of PSII complexes outside the grana and subsequent mixing. Rather, it is supportive of the notion made above that they move en block with the grana layers.

The second set of experiments employed scanning electron microscopy. Similar to the results obtained by confocal microscopy, the images, recorded at the three stages of the experiments (Figures 6A to 6C), revealed that the transitions were largely, but not fully, reversible. The grana regained their structure in ~90% of the chloroplasts that were adapted back to state I. The diameter of the grana in these chloroplasts was restored to within ~10% of that measured for state I–adapted chloroplasts that were not induced to undergo the transition to state II. The base area of the chloroplasts, however, did not return to its state I value, suggesting that large-scale rearrangements in the network during the reverse transition were partially impaired.

DISCUSSION

The primary physiological driving force for the segregation of higher-plant thylakoid membranes into granal and stroma lamellar domains is unknown (for recent reviews, see Chow et al., 2005; Mullineaux, 2005). Nevertheless, the balance between the two morphological domains likely plays important roles in the steady state function of thylakoids as well as in their ability to adapt to transient or long-term changes in light conditions.

Several studies showed that isolated thylakoids undergo massive reorganization when subjected to low-salt solutions (see Izawa and Good, 1966; Murakami and Packer, 1971). These conditions are believed to mimic, at least to some extent, the structural alterations of thylakoids following photoinduced phosphorylation of LHCII (Georgakopoulos and Argyroudi-Akoyunoglou, 1994, 1997; Stys, 1995; Chow, 1999). Grana in such experiments underwent complete or nearly complete unstacking and no longer resembled the stacked, tightly appressed morphology of dark-adapted thylakoids. Similar rearrangements were observed for divalent cation–depleted de-enveloped chloroplasts by AFM analysis (Kaftan et al., 2002). It has also been proposed

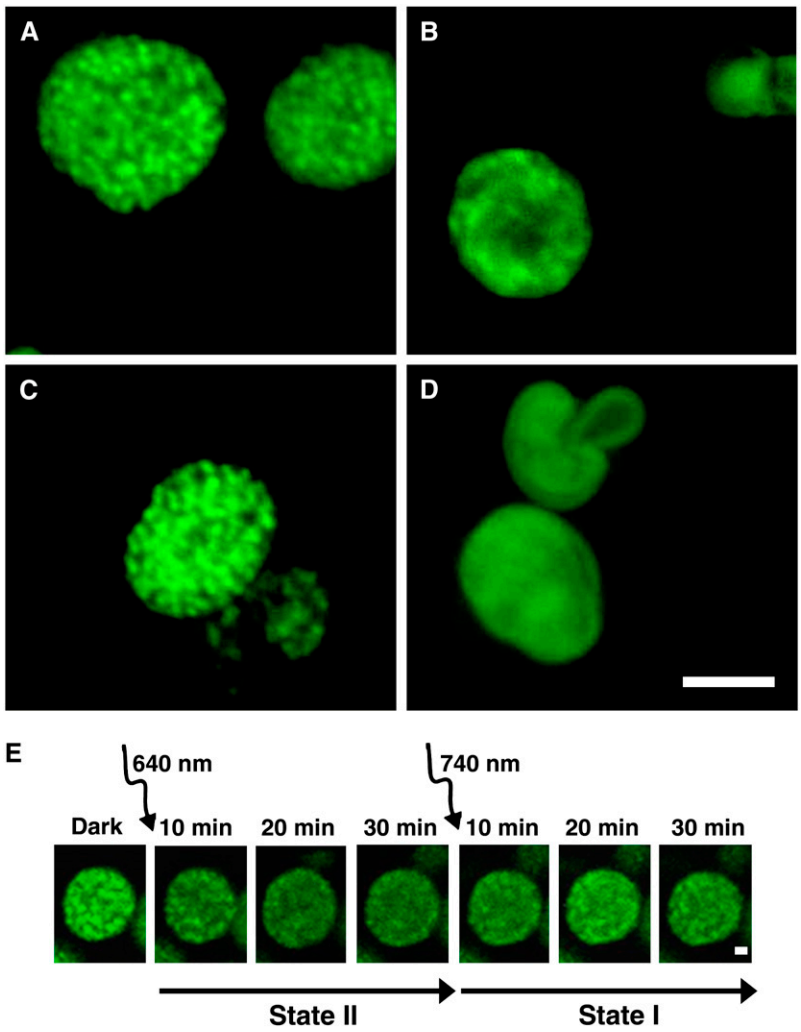

Figure 5. Confocal Microscopy of Structural Alterations in Native Hydrated De-Enveloped Chloroplasts during State Transitions.

Fluorescence is shown in pseudocolor. **(A)** to **(D)** show representative images of thylakoids subjected to different treatments.
(A) Dark-adapted chloroplasts.
(B) and **(C)** Dark-adapted chloroplasts subjected to PSII-specific light in the presence **(B)** or absence **(C)** of ATP.
(D) Dark-adapted chloroplasts treated with 1 mM duroquinol, in the dark. Samples in **(A)**, **(B)**, and **(D)** were incubated in the presence of 1 mM ATP and 10 mM NaF; 10 μM DCMU was added just prior to imaging. For **(C)**, DCMU was added as in **(A)**, **(B)**, and **(D)**. Bar = 5 μm.
(E) Time-lapse series of dark-adapted chloroplasts subjected first to PSII-specific light and then to PSI-specific light. Samples contained 1 mM ATP, 10 μM ferredoxin, and 0.6 mM $NADP^+$. Bar = 1 μm. Similar results were obtained in the presence of 20 μM gramicidin D (see Supplemental Figure 2 online).

that grana unstacking, induced by cation depletion, and the rearrangements that follow are accompanied by mixing of the previously segregated photosystems within the membranes (Staehelin, 1976; Barber, 1980). Subsequent studies suggested that LHCII phosphorylation at low Mg^{2+} concentrations results in nonspecific membrane unstacking, leading to intermixing of the two photosystems (Horton and Black, 1983; Telfer et al., 1984), which likely does not occur under light-induced state transitions (Staehelin and Van der staay, 1996).

In contrast with the above, other studies have shown that the structural alterations that occur in thylakoid membranes during light-induced state transitions are quite limited (see Drepper et al., 1993; Mustardy and Garab, 2003; Shimoni et al., 2005). Specifically, it was noted that the difference in membrane stacking between the two states, in vivo, does not exceed 10 to 20% (Kyle et al., 1983; Rozak et al., 2002) and that structural rearrangements are mostly confined to grana margins (Drepper et al., 1993). It was also shown that excessive unstacking by means of cation depletion is associated with lesions and ruptures of the membranes (Brangeon, 1974; Briantais et al., 1984) and may lead to irreversible changes in the structure of the granum-stroma assembly or in the organization of PSII-LHCII arrays within it (Brangeon, 1974; Briantais et al., 1984; Garab et al., 1991; Shimoni et al., 2005).

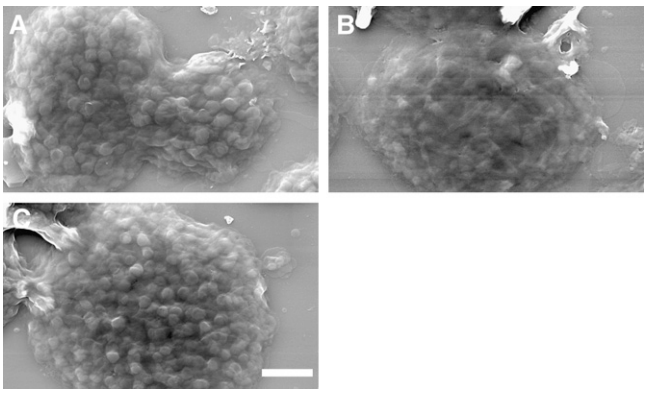

Figure 6. Reversibility of the Structural Changes Occurring in Isolated Thylakoids during State Transitions Monitored by Scanning Electron Microscopy.

(A) A chloroplast adapted to state I by exposure to PSI-specific light.
(B) A chloroplast treated as in **(A)** but subsequently induced to undergo transition to state II.
(C) A chloroplast treated as in **(B)** but resubjected to PSI light to undergo back-transition to state I. Samples were incubated in the presence of 10 μM ferredoxin, 0.6 mM $NADP^+$, 20 μM gramicidin D, and 1 mM ATP; NaF (10 mM) was added at the end of each illumination cycle. Bar = 2 μm.

Traditionally, the structure of the granum-stroma assembly, which constitutes the basic unit of higher-plant thylakoid networks, is thought to be stabilized by multiple interactions and forces. These include van der Waals forces, dipole–dipole interactions, entropic forces, as well as steric hindrances and short- and long-range lipid-mediated interactions that govern the lateral segregation of protein complexes within the membranes (reviewed in Barber, 1982; Stys, 1995; Pali et al., 2003; Chow et al., 2005; Dekker and Boekema, 2005; Kim et al., 2005). Changes in membrane architecture have been accordingly interpreted in terms of perturbations in the balance of these forces (e.g., those caused by the movement of LHCII complexes between the two thylakoid domains during state transitions). However, this view was formulated when the three-dimensional organization of the granum-stroma assembly was unknown. This structure has only recently become available from an electron microscope tomography study performed on state I–adapted cryo-fixed leaves (Shimoni et al., 2005). The structure revealed that, in this state, the granum layers are physically connected to each other and to the surrounding stroma lamellae. As shown in Figure 7A, the grana are made, in essence, by bifurcations of stroma lamellar sheets into adjacent layers that run roughly parallel to each other. These layers or discs bend at their edges, near the bifurcation points, and fuse with each other through membrane bridges that run at a small angle to the long axis of the granum cylinder (two such bridges are shown in the figure). Thus, significant alterations in the structure of the grana and, hence, in the thylakoid network cannot take place without breakage or reformation of the lateral and/or vertical connections that stabilize the grana. This holds for state transitions or for any other adaptation processes that are associated with structural reorganization of the thylakoid membranes.

This study has two key observations, the first of which is that the structural rearrangements in chloroplast thylakoid membranes during state transitions, albeit not reaching the extent observed upon salt-induced membrane unstacking, are large scale. These include macroscopic changes in the shape of the thylakoid network, an increase in membrane deformability, as

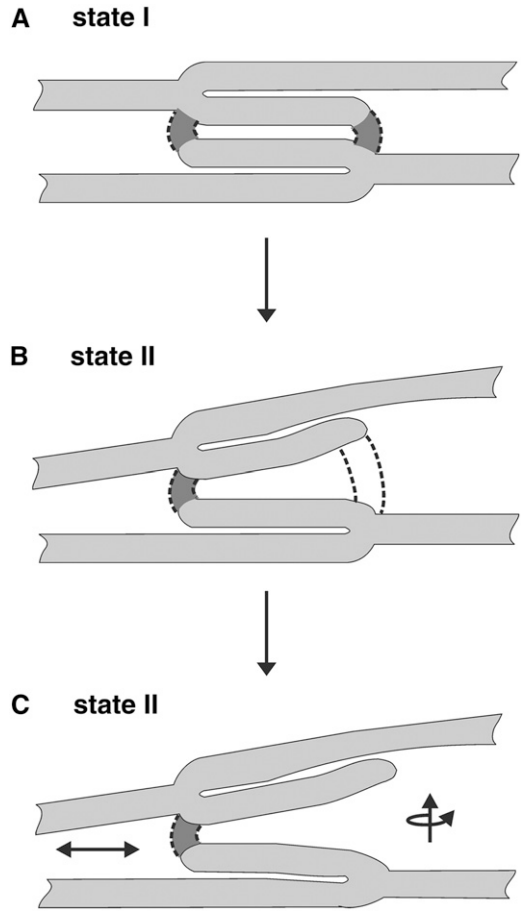

Figure 7. Model for the Structural Rearrangements in the Granum-Stroma Assembly during State I → State II Transition.

(A) Structure of the granum-stroma assembly in state I. The granum is composed of paired layers that are formed by bifurcations of stroma lamellar sheets. These layers are interconnected by membrane bridges (indicated as darker regions delimited by dashed lines) that emerge from one layer and fuse to the other. In reality, the two bridges shown may not appear in the same cross section.
(B) and **(C)** Remodeling of the assembly upon transition to state II. Consequent to LHCII migration from the grana to the stroma lamellae, the margins of the granum body become unstable and adjacent layers retract from each other at the edges of the granum body. This movement subjects the internal grana bridges to strain **(B)**. Once a critical threshold is reached, some of the bridges break **(C)**. The subsequent events are less clear but probably involve rotation and vertical and lateral movements (arrows) of the layers where breakage occurred. These motions cause a shape transition, leading to unstacking and partial disassembly of the granum. Restoration of the grana stacks during the reverse transition (state II → state I) requires reformation of the membrane bridges that interconnect neighboring layers in the granum.

well as unstacking and fragmentation of the grana, which resulted in partial loss of granum structure. The alterations in membrane architecture were largely reversible and are qualitatively similar to those reported for thylakoid membranes of algal (*Phaeocystis antartica*) cells exposed to low and high levels of light (Moisan et al., 2006).

The second observation is that, topologically, the aforementioned alterations of the thylakoid network require that some of the lateral and/or vertical connections that stabilize the granum-stroma assembly be broken. Figure 7 shows a model we propose for the rearrangement of the assembly during the transition from state I to state II; generally, the back-transition is taken to be a reversal of this process. We assume that phosphorylation of LHCII is initiated at regions near the grana-stroma interface. The subsequent migration of the phosphorylated antennae to the stroma lamellae disrupts the attractive interactions between neighboring layers at the margins, causing adjacent layers to retract from each other at the edges of the granum. It also leads to local changes in the highly curved regions that constitute the grana margins. Curved membrane domains are known to be sites where fission and fusion processes occur and require a specific lipid and/or protein composition (see Dekker and Boekema, 2005; Atilgan and Sun, 2007; Voeltz and Prinz, 2007 and references therein). We propose that the transit of LHCII (perhaps with bound lipids) from the grana to the stroma lamellae alters the local composition of lipids and/or proteins at the margins, leading to their destabilization. The latter, together with the retraction of the layers at the granum edges, subject the vertical and lateral connections to an increasing strain (Figure 7B), which, once reaching a critical threshold, causes some of the connections to break (Figure 7C). The fraction of bridges that break during the transition is unknown, yet it must be limited, as complete breakage would lead to destruction of the grana and to massive damage to the membranes, as observed upon exposure of thylakoids to low-ionic-strength solutions. Such injuries may thus reflect an extreme case where breakage of the membrane bridges that stabilize the granum-stroma assembly proceeds in an uncontrollable manner.

Following the aforementioned localized events, the grana undergo additional rearrangements that eventually lead to remodeling of the entire membrane network. These rearrangements likely commence at the grana and include retraction of neighboring layers along the granum axis, as well as rotational and/or lateral movements that displace some of the layers out of the granum body. The outcome of these translational and rotational movements is unstacking and fragmentation of the grana, which consequently appear staggered and distorted. The displacement of layers out of the granum body also gives rise to the hybrid lamellae that possess features of both stromal and granal thylakoids observed in state II–adapted networks. The alterations in granum structure then propagate throughout the entire lamellar system, bringing about global changes in network dimensions and appearance. The pathways by which these macroscopic changes proceed are unknown, but we believe that they reflect relaxations of strains induced in the stroma lamellar sheets by the movements of grana layers, to which they are connected. As indicated in Figure 5E, these relaxations are relatively slow, taking ~20 min to complete.

Breakage of the lateral and/or vertical connections of the layers in the grana, during state I → state II transition, and their reformation during the reverse transition, are presumably associated with significant energy barriers. In biological membranes, overcoming these barriers typically requires dedicated protein machineries that stabilize transition states in the fission/fusion process (e.g., like those operating in the mitochondria, the Golgi apparatus, and the endoplasmic reticulum) (Misteli and Warren, 1995; Dekker and Boekema, 2005; Mannella, 2006; Atilgan and Sun, 2007; Voeltz and Prinz, 2007). Proteins involved in membrane remodeling, namely FZL, VIPP1, and Thf1, have been identified in chloroplasts and were shown to associate with thylakoids (Li et al., 1994; Kroll et al., 2001; Wang et al., 2004; Gao et al., 2006). These and/or hitherto unidentified proteins may participate in the breakage and restoration of the interlayer granal bridges during state transitions as well as during network development and long-term acclimation.

METHODS

Plants

Arabidopsis thaliana (ecotype Columbia-0) was used in all experiments. Plants were grown in a commercial potting mixture (Hummert International) at 20°C, with a 16/8 h light/dark period, and were dark-adapted overnight before use.

Preparation of De-Enveloped Chloroplasts

Envelope-free chloroplasts were prepared according to Casazza et al. (2001), with a few modifications. Rosette leaves from 3- to 4-week-old plants were harvested just before efflorescence and were floated on ice-cold water for 30 min in the dark and then blotted dry. All successive steps were performed in the dark on ice. Following blotting, the leaves (3 to 4 g) were blended in grinding buffer (20 mL) containing 0.4 M sorbitol, 5 mM EDTA, 5 mM EGTA, 5 mM $MgCl_2$, 10 mM $NaHCO_3$, 20 mM Tricine, pH 8.4, and 0.5% (w/v) fatty acid–free BSA, which was prepared according to Arion and Racker (1970). The slurry was filtered through eight layers of cheesecloth and centrifuged for 3 min at 2600*g* (4°C). The supernatant was discarded, and half of the pellet (topmost) was suspended in resuspension buffer (RB; 10 mL) containing 0.3 M sorbitol, 2.5 mM EDTA, 5 mM $MgCl_2$, 10 mM $NaHCO_3$, 20 mM HEPES, pH 7.6, and 0.5% (w/v) fatty acid–free BSA. After two successive centrifugation steps (2600*g* for 3 min, at 4°C), the pellet was resuspended for 5 min in hypotonic buffer (5 mL) containing 2.5 mM EDTA, 5 mM $MgCl_2$, 10 mM $NaHCO_3$, 20 mM HEPES, pH 7.6, and 0.5% (w/v) fatty acid–free BSA. The suspension was centrifuged for 3 min at 200*g* (4°C), and the supernatant was collected. The pellet formed by centrifugation of the supernatant (2600*g* for 3 min, at 4°C) contained the de-enveloped chloroplasts. The thylakoid membranes were resuspended in RB (see note below) and were used for experiments within 2 h of isolation. The chlorophyll concentration in the preparations was determined according to Porra et al. (1989).

The photochemical activity of the de-enveloped chloroplasts was evaluated by measuring the maximal photochemical yield of PSII, Φ_p^{max}, and the rate of linear electron transport from H_2O to $NADP^+$, as reflected by the rate of oxygen evolution. Φ_p^{max} was determined from measurements of chlorophyll fluorescence using an FL-100 double-modulation fluorometer (Photon Systems Instruments). Oxygen evolution was measured in cell of a Clark-type electrode at 25°C, under red light illumination (640 nm), in the presence of 20 μM ferredoxin and 1 mM $NADP^+$.

Induction and Validation of State Transitions

State I was induced by overnight incubation of the plants in the dark or by subjecting thylakoids to PSI-specific light using light-emitting diodes (740 ± 35 nm). In the latter case, thylakoid membranes (100 μg of Chl·mL^{-1}) were suspended in RB supplemented with 10 μM ferredoxin, 0.6 mM $NADP^+$, 20 μM gramicidin D, and 1 mM ATP. Before use, the membranes were assayed for oxygen evolution to verify that ferredoxin $NADP^+$ reductase was not damaged during isolation. State II was induced by subjecting thylakoids (100 μg of Chl·mL^{-1} in RB supplemented with 1 mM ATP) either to PSII-specific light or to 1 mM duroquinol (in the dark) (Zer et al., 1999). PSII-specific light was provided by a halogen lamp (KL 1500 electronic; Zeiss) and was passed through a 640-nm interference filter (20-nm half-bandwidth). When required, phosphatase activity was inhibited by the addition of 10 mM NaF (Bennett, 1983). The photon flux density reaching the samples was measured using a Li-189 radiometer (Li-Cor).

Validation of state transitions was assessed by low-temperature and room-temperature chlorophyll fluorescence measurements and by monitoring the phosphorylation levels of LHCII. Low-temperature emission spectra of thylakoid membrane suspensions, excited at 480 nm, were recorded in liquid nitrogen (77K) using an SLM-Aminco 8100 spectrofluorometer. Room-temperature fluorescence measurements were performed using a pulse amplitude modulation fluorometer (Walz). Phosphorylation of the LHCII proteins, Lhcb1 and Lhcb2, was assayed by protein gel blotting as described (Rintamaki et al., 1997) using phosphothreonine-specific antiserum (Cell Signaling Technology) and was quantified by densitometry.

Earlier works on pea (*Pisum sativum*) chloroplasts indicated that LHCII phosphorylation in the presence of Mg^{2+} concentrations below 5 mM may lead to membrane unstacking, which is not solely due to antennae migration from granal to stroma lamellar domains (Horton and Black, 1983; Telfer et al., 1984). We therefore performed scanning electron microscopy analysis of samples resuspended in buffers (RB) containing effective Mg^{2+} concentrations of 5 and 8 mM, in addition to our working 2.5 mM concentration. As can be seen (see Supplemental Figure 3 online), within this range, the Mg^{2+} concentration does not affect the morphology of the thylakoids and does not affect the structural rearrangements that occur during their transition from state I to state II.

AFM

Glass cover slips were coated with 0.01% (w/v) poly-L-lysine. Samples were adsorbed onto the cover slips by gentle centrifugation (5 min at 1000*g*), fixed in RB containing 2% (v/v) glutaraldehyde and 3% (v/v) paraformaldehyde, and rinsed three times with RB. Samples were then washed with distilled water and air-dried. Recordings were made in contact mode with the PicoSPM (Molecular Imaging) equipped with a 30-μm scanner, using oxide-sharpened Si_3N_4 cantilevered tips (k = 0.1 N/m; Digital Instruments). Images were acquired with forces set minimally above lift-off values, at 1 to 2 Hz.

Scanning Electron Microscopy

Samples were adsorbed onto silicon chips and fixed with 2% (v/v) glutaraldehyde and 3% (v/v) paraformaldehyde in RB. Following coating with Cr film (Emitech K575X), samples were viewed with an XL30 ESEM FEG scanning electron microscope (FEI) operating at 10 kV.

Transmission Electron Microscopy

Samples were fixed with 2% (v/v) glutaraldehyde and 3% (v/v) paraformaldehyde in RB for 1 h and were suspended in 1.7% molten agarose at 37°C for 15 min. The samples were centrifuged and the sediment left on ice for gelling of the agarose. They were then post-fixed with 1% (w/v) osmium tetraoxide in a buffer containing 0.1 M Na-cacodylate, pH 7.4, 5 mM $CaCl_2$, 0.5% $K_2CR_2O_7$, and 0.5% $K_4[Fe(CN)_6]$ for 1 h, rinsed with double-distilled water, and stained with 2% (w/v) uranyl acetate. Samples were then dehydrated by a graded series of ethanol and embedded in Epon (Electron Microscopy Sciences); blocks were polymerized overnight at 60°C. Thin sections (50 to 70 nm) were cut using an Ultracut microtome (Leica), post-stained with uranyl acetate and lead citrate, and examined with a Tecnai T12 transmission electron microscope (FEI) operating at 120 kV.

Confocal Laser Scanning Microscopy

Fluorescence images of photosynthetically active de-enveloped chloroplasts were acquired with an Olympus FluoView 500 confocal laser scanning microscope (IX70-based) using a PlanApo oil-immersion objective (×60; numerical aperture of 1.4). Samples were visualized with a He-Ne laser (λ_{ex} = 543 nm) and a >660-nm high-pass filter. For each specimen, a focal series was collected at 0.3-μm steps. Where indicated, measurements were made in the presence of 10 μM DCMU. For time-lapse microscopy, the sample was placed on a cover slip at a vertical position that is out of focus of the condenser of the confocal microscope, allowing for wide-angle illumination through the condenser. State II was induced by illumination with light from a halogen lamp that was passed through a 640-nm interference filter with a half bandwidth of 20 nm. This illumination scheme was replaced with a light-emitting diode at 740 ± 35 nm, filtered by a high-pass filter with a cutoff wavelength of 695 nm to induce state I. Photon flux density at the sample was measured by replacing the objective with a Li-189 radiometer (Li-Cor).

Image Processing and Statistical Analysis

Images were processed and analyzed using Analysis (Soft Imaging System) and MATLAB (The Mathworks). Statistical significance of differences in geometric properties of thylakoids trapped in state I or in state II was determined by one-way analysis of variance tests complemented by Tukey's multiple comparisons of means with significance set at 0.05. Sample size was 6 to 15 chloroplasts and 60 to 140 grana. Statistical analyses were performed using Origin and MATLAB.

Supplemental Data

The following materials are available in the online version of this article.

Supplemental Figure 1. Changes in Chlorophyll Fluorescence during State Transitions Measured at Room Temperature.

Supplemental Figure 2. Reversibility of the Structural Rearrangements during State Transitions as Monitored by Confocal Microscopy.

Supplemental Figure 3. Scanning Electron Microscopy Images of State I– and State II–Adapted Thylakoids Resuspended in Buffers Containing Increasing Mg^{2+} Concentrations.

ACKNOWLEDGMENTS

We thank Eyal Tamary for his help in the confocal imaging experiments. This research was supported by grants from the Henry Legrain Foundation (E.S.), from the Avron-Even-Ari Minerva Center for Photosynthesis Research (I.O.), and from the Israel Science Foundation and the Avron-Wilstätter Minerva Center for Photosynthesis Research (Z.R.).

Received September 25, 2007; revised March 12, 2008; accepted March 20, 2008; published April 8, 2008.

REFERENCES

Allen, J.F. (1992a). Protein-phosphorylation in regulation of photosynthesis. Biochim. Biophys. Acta **1098:** 275–335.

Allen, J.F. (1992b). How does protein phosphorylation regulate photosynthesis? Trends Biochem. Sci. **17:** 12–17.

Allen, J.F., and Forsberg, J. (2001). Molecular recognition in thylakoid structure and function. Trends Plant Sci. **6:** 317–326.

Anderson, J.M. (1999). Insights into the consequences of grana stacking of thylakoid membranes in vascular plants: A personal perspective. Aust. J. Plant Physiol. **26:** 625–639.

Arion, W.J., and Racker, E. (1970). Partial resolution of the enzymes catalyzing oxidative phosphorylation. 23. Preservation of energy coupling in submitochondrial particles lacking cytochrome oxidase. J. Biol. Chem. **245:** 5186–5194.

Aro, E.M., and Ohad, I. (2003). Redox regulation of thylakoid protein phosphorylation. Antioxid Redox Signal. **5:** 55–67.

Arvidsson, P.O., and Sundby, C. (1999). A model for the topology of the chloroplast thylakoid membrane. Aust. J. Plant Physiol. **26:** 687–694.

Atilgan, E., and Sun, S.X. (2007). Shape transitions in lipid membranes and protein mediated vesicle fusion and fission. J. Chem. Phys. **126:** 095102.

Barber, J. (1980). An explanation for the relationship between salt-induced thylakoid stacking and the chlorophyll fluorescence changes associated with changes in spillover of energy from photosystem-II to photosystem-I. FEBS Lett. **118:** 1–10.

Barber, J. (1982). Influence of surface-charges on thylakoid structure and function. Annu. Rev. Plant Physiol. **33:** 261–295.

Bennett, J. (1983). Thylakoid protein phosphorylation during state 1-state 2 transitions in osmotically shocked pea chloroplasts. Biochim. Biophys. Acta **722:** 176–181.

Brangeon, J. (1974). Structural modifications in lamellar system of isolated *Zea mays* chloroplasts under different ionic conditions. J. Microsc. Oxford **21:** 75–84.

Briantais, J.M., Vernotte, C., Olive, J., and Wollman, F.A. (1984). Kinetics of cation-induced changes of photosystem-II fluorescence and of lateral distribution of the 2 photosystems in the thylakoid membranes of pea chloroplasts. Biochim. Biophys. Acta **766:** 1–8.

Casazza, A.P., Tarantino, D., and Soave, C. (2001). Preparation and functional characterization of thylakoids from *Arabidopsis thaliana.* Photosynth. Res. **68:** 175–180.

Chow, W.S. (1999). Grana formation: Entropy-assisted local order in chloroplasts? Aust. J. Plant Physiol. **26:** 641–647.

Chow, W.S., Kim, E.H., Horton, P., and Anderson, J.M. (2005). Granal stacking of thylakoid membranes in higher plant chloroplasts: The physicochemical forces at work and the functional consequences that ensue. Photochem. Photobiol. Sci. **4:** 1081–1090.

Dekker, J.P., and Boekema, E.J. (2005). Supramolecular organization of thylakoid membrane proteins in green plants. Biochim. Biophys. Acta **1706:** 12–39.

Drepper, F., Carlberg, I., Andersson, B., and Haehnel, W. (1993). Lateral diffusion of an integral nembrane protein - Monte Carlo analysis of the migration of phosphorylated light-harvesting complex-II in the thylakoid membrane. Biochemistry **32:** 11915–11922.

Gao, H., Sage, T.L., and Osteryoung, K.W. (2006). FZL, an FZO-like protein in plants, is a determinant of thylakoid and chloroplast morphology. Proc. Natl. Acad. Sci. USA **103:** 6759–6764.

Garab, G., Kieleczawa, J., Sutherland, J.C., Bustamante, C., and Hind, G. (1991). Organization of pigment protein complexes into macrodomains in the thylakoid membranes of wild-type and chlorophyll-B-less mutant of barley as revealed by circular dichroism. Photochem. Photobiol. **54:** 273–281.

Garab, G., and Mustardy, L. (1999). Role of LHCII-containing macrodomains in the structure, function and dynamics of grana. Aust. J. Plant Physiol. **26:** 649–658.

Georgakopoulos, J.H., and Argyroudi-Akoyunoglou, J.H. (1994). Release of a light thylakoid membrane fragment with high F-730/F-685 fluorescence emission ratio (77-K) by digitonin disruption from low-salt-destacked or phosphorylated thylakoids of pea. J. Photochem. Photobiol. B **26:** 57–65.

Georgakopoulos, J.H., and Argyroudi-Akoyunoglou, J.H. (1997). Implication of D1 degradation in phosphorylation-induced state transitions. Photosynth. Res. **53:** 185–195.

Govindjee (1995). 63 Years since Kautsky - Chlorophyll-a fluorescence. Aust. J. Plant Physiol. **22:** 131–160.

Haldrup, A., Jensen, P.E., Lunde, C., and Scheller, H.V. (2001). Balance of power: A view of the mechanism of photosynthetic state transitions. Trends Plant Sci. **6:** 301–305.

Horton, P., and Black, M.T. (1983). A comparison between cation and protein-phosphorylation effects on the fluorescence induction curve in chloroplasts treated with 3-(3,4-dichlorophenyl)-1,1-dimethylurea. Biochim. Biophys. Acta **722:** 214–218.

Izawa, S., and Good, N.E. (1966). Effect of salts and electron transport on conformation of isolated chloroplasts. 2. Electron microscopy. Plant Physiol. **41:** 544–552.

Kaftan, D., Brumfeld, V., Nevo, R., Scherz, A., and Reich, Z. (2002). From chloroplasts to photosystems: In situ scanning force microscopy on intact thylakoid membranes. EMBO J. **21:** 6146–6153.

Kim, E.H., Chow, W.S., Horton, P., and Anderson, J.M. (2005). Entropy-assisted stacking of thylakoid membranes. Biochim Biophys Acta. **1708:** 187–195.

Kroll, D., Meierhoff, K., Bechtold, N., Kinoshita, M., Westphal, S., Vothknecht, U.C., Soll, J., and Westhoff, P. (2001). VIPP1, a nuclear gene of Arabidopsis thaliana essential for thylakoid membrane formation. Proc. Natl. Acad. Sci. USA **98:** 4238–4242.

Kruse, O. (2001). Light-induced short-term adaptation mechanisms under redox control in the PSII-LHCII supercomplex: LHC II state transitions and PSII repair cycle. Naturwissenschaften **88:** 284–292.

Kyle, D.J., Staehelin, L.A., and Arntzen, C.J. (1983). Lateral mobility of the light-harvesting complex in chloroplast membranes controls excitation energy distribution in higher plants. Arch. Biochem. Biophys. **222:** 527–541.

Li, H.M., Kaneko, Y., and Keegstra, K. (1994). Molecular-cloning of a chloroplastic protein associated with both the envelope and thylakoid membranes. Plant Mol. Biol. **25:** 619–632.

Mannella, C.A. (2006). The relevance of mitochondrial membrane topology to mitochondrial function. Biochim. Biophys. Acta **1762:** 140–147.

Maxwell, K., and Johnson, G.N. (2000). Chlorophyll fluorescence – A practical guide. J. Exp. Bot. **51:** 659–668.

Misteli, T., and Warren, G. (1995). Mitotic disassembly of the Golgi apparatus in vivo. J. Cell Sci. **108:** 2715–2727.

Moisan, T.A., Ellisman, M.H., Buitenhuys, C.W., and Sosinsky, G.E. (2006). Differences in chloroplast ultrastructure of *Phaeocystis antarctica* in low and high light. Mar. Biol. **149:** 1281–1290.

Mullineaux, C.W. (2005). Function and evolution of grana. Trends Plant Sci. **10:** 521–525.

Mullineaux, C.W., and Emlyn-Jones, D. (2005). State transitions: An example of acclimation to low-light stress. J. Exp. Bot. **56:** 389–393.

Murakami, S., and Packer, L. (1971). Role of cations in organization of chloroplast membranes. Arch. Biochem. Biophys. **146:** 337–347.

Mustardy, L., and Garab, G. (2003). Granum revisited. A three-dimensional model where things fall into place. Trends Plant Sci. **8:** 117–122.

Nir, I., and Pease, D.C. (1973). Chloroplast organization and ultrastructural

localization of photosystems I and II. J Ultrastruct Res. **42:** 534–550.

Pali, T., Garab, G., Horvath, L.I., and Kota, Z. (2003). Functional significance of the lipid-protein interface in photosynthetic membranes. Cell. Mol. Life Sci. **60:** 1591–1606.

Porra, R.J., Thompson, W.A., and Kriedemann, P.E. (1989). Determination of accurate extinction coefficients and simultaneous equations for assaying chlorophyll a and chlorophyll b extracted with 4 different solvents - Verification of the concentration of chlorophyll standards by atomic-absorption spectroscopy. Biochim. Biophys. Acta **975:** 384–394.

Rintamaki, E., Salonen, M., Suoranta, U.M., Carlberg, I., Andersson, B., and Aro, E.M. (1997). Phosphorylation of light-harvesting complex II and photosystem II core proteins shows different irradiance-dependent regulation in vivo. Application of phosphothreonine antibodies to analysis of thylakoid phosphoproteins. J. Biol. Chem. **272:** 30476–30482.

Rochaix, J.D. (2007). Role of thylakoid protein kinases in photosynthetic acclimation. FEBS Lett. **581:** 2768–2775.

Rozak, P.R., Seiser, R.M., Wacholtz, W.F., and Wise, R.R. (2002). Rapid, reversible alterations in spinach thylakoid appression upon changes in light intensity. Plant Cell Environ. **25:** 421–429.

Ryrie, I.J. (1983). Freeze-fracture analysis of membrane appression and protein segregation in model membranes containing the chlorophyll-protein complexes from chloroplasts. Eur. J. Biochem. **137:** 205–213.

Shimoni, E., Rav-Hon, O., Ohad, I., Brumfeld, V., and Reich, Z. (2005). Three-dimensional organization of higher-plant chloroplast thylakoid membranes revealed by electron tomography. Plant Cell **17:** 2580–2586.

Staehelin, L.A. (1976). Reversible particle movements associated with unstacking and restacking of chloroplast membranes in vitro. J. Cell Biol. **71:** 136–158.

Staehelin, L., and Van der staay, G. (1996). Structure, composition, functional organization and dynamic properties of thylakoid membranes. In Oxygenic Photosynthesis: The Light Reactions, D.R. Ort and C.F. Yocum, eds (Dordrecht, The Netherlands: Kluwer Academic Publishers), pp. 11–30.

Stys, D. (1995). Stacking and separation of photosystem I and photosystem II in plant thylakoid membranes: A physico-chemical view. Physiol. Plant. **95:** 651–657.

Telfer, A., Hodges, M., Millner, P.A., and Barber, J. (1984). The cation-dependence of the degree of protein phosphorylation-induced unstacking of pea thylakoids. Biochim. Biophys. Acta **766:** 554–562.

Voeltz, G.K., and Prinz, W.A. (2007). Sheets, ribbons and tubules - How organelles get their shape. Nat. Rev. Mol. Cell Biol. **8:** 258–264.

Wang, Q., Sullivan, R.W., Kight, A., Henry, R.L., Huang, J.R., Jones, A.M., and Korth, K.L. (2004). Deletion of the chloroplast-localized thylakoid formation1 gene product in Arabidopsis leads to deficient thylakoid formation and variegated leaves. Plant Physiol. **136:** 3594–3604.

Wollman, F.A. (2001). State transitions reveal the dynamics and flexibility of the photosynthetic apparatus. EMBO J. **20:** 3623–3630.

Zer, H., Vink, M., Keren, N., Dilly-Hartwig, H.G., Paulsen, H., Herrmann, R.G., Andersson, B., and Ohad, I. (1999). Regulation of thylakoid protein phosphorylation at the substrate level: Reversible light-induced conformational changes expose the phosphorylation site of the light-harvesting complex II. Proc. Natl. Acad. Sci. USA **96:** 8277–8282.

Zer, H., Vink, M., Shochat, S., Herrmann, R.G., Andersson, B., and Ohad, I. (2003). Light affects the accessibility of the thylakoid light harvesting complex II (LHCII) phosphorylation site to the membrane protein kinase(s). Biochemistry. **42:** 728–738.